International Conference on Applied Energy 2020
Dec. 1 - Dec. 10, 2020, Bangkok / Virtual
Paper ID: 559

An investigation on mitigation of thermal runaway of lithium-ion batteries using thermal barrier

Caixing Chen[a], Huichang Niu[a], Zhao Li[a], Lei Li[a], Yi Zhu[a], Xi Jiang[b]
[a]Institute of Industry Technology, Guangzhou & Chinese Academy of Sciences, Guangzhou, 511458, China
[b] School of Engineering & Materials Science, Queen Mary University of London, London E1 4NS, UK

ABSTRACT

Applying thermal barrier between batteries is one of the most effective method to mitigate thermal runaway (TR) of battery. This work investigated TR of a single battery considering the contact resistance between the battery internal cell and external hard shell, and TR mitigation using equivalent thermal barrier between batteries. The results indicate the contact resistance between the internal cell and external shell is around 0.0207 $m^2 \cdot K \cdot W^{-1}$. For preventing TR propagation, resistance of thermal barrier should be higher than 0.01242 $m^2 \cdot K \cdot W^{-1}$.

Keywords: Thermal runaway, propagation, mitigation, thermal barrier, simulation.

1. INTRODUCTION

Lithium-ion batteries (LiBs) have been widely used in electric vehicles (EV) and electric-chemical energy storage systems due to their high energy density and long cycle life. However, fire accidents of electric vehicles, caused by thermal runaway (TR) of batteries, present significant threats to lives and safe design of battery systems [1]. Although lots of efforts have been paid to TR of batteries, it is still a difficult task to eliminate the risk [2]. To avoid large-scale battery fires or mitigate fire hazards, understanding the TR mechanisms and propagation processes in a module is a necessity.

For tightly arranged prismatic battery modules, heat conduction through battery shell was considered as the dominant heat transfer mode. Feng et al. [3] conducted heat transfer analysis during the TR propagation process in a 6-battery module. It is found that fire had little influence on TR propagation, and only 12% of the total heat released from a single battery was enough to trigger the adjacent battery to TR, mainly by heat conduction through battery shell. Hence, mitigating TR propagation by applying thermal barrier between batteries, is one of the most effective methods [4].

The heat energy, transferred between batteries, originates from exothermic reactions during the TR of a battery. Researchers have developed some TR models describing the TR processes. Ping et al. [5] identified thermal behavior of both single electrode system and full cell system, and calculated the separate kinetics using deconvolution method. A multistep TR thermodynamic model was then developed and validated [6]. Ren et al. [7] revealed that six exothermic reactions were the dominant heat sources. By coupling all the exothermic reactions, a TR model based on kinetics parameters of each exothermic reaction was developed. Feng et al. [8] constructed a 3D TR model, in which chemical kinetics for TR was simplified with empirical equations. Simulations of TR propagation triggered by nail penetration were also conducted. Previous works on TR modeling help understanding the detailed TR processes, and provide theoretical basis for quantifying heat generation of LiBs that undergoing TR. Developing a numerical method on heat transfer analysis and mitigation of TR propagation of LiBs by thermal barrier becomes feasible.

In this work, a TR model is built for LiBs with $Li(Ni_{0.5}Co_{0.2}Mn_{0.3})O_2$ cathode, then a heat transfer analysis is conducted with special attention to the contact thermal resistance between cells (internal component) and hard shells (usually made of aluminum or iron). In addition, TR propagation between modules is numerically simulated, and the critical equivalent thermal barrier between batteries that could mitigate TR propagation is discussed.

2. MODEL DESCRIPTION AND VALIDATION

2.1 Battery and module description

Commercial prismatic LiBs (anode: graphite, cathode: $Li(Ni_{0.5}Co_{0.2}Mn_{0.3})O_2$) with nominal capacity of

Selection and peer-review under responsibility of the scientific committee of the 12th Int. Conf. on Applied Energy (ICAE2020).

13.5 Ah and size of 110.5 mm×68 mm×15 mm were used. Thickness of the external aluminum shell is 0.45 mm. LiB modules were constructed with 5 tightly packed batteries. All LiBs were 100% charged before tests.

2.2 Heat source of TR

The total heat Q (t) released from a TR LiB can be calculated by the following equation

$$Q(t) = Q_{chem}(t) + Q_{ele}(t) - Q_{vent}(t) - Q_h(t) \quad (1)$$

where Q_{chem}, Q_{ele}, Q_{vent}, and Q_h denote heat related with chemical reactions, internal short circuit, opening of safety vent, and dissipated heat to environment, respectively. $Q_{chem}(t)$ is sum of the heats generated by decomposition of SEI (Q_{SEI}), anode, separator, electrolyte, and cathodes, given as

$$Q_{chem}(t) = Q_{SEI}(t) + Q_{seperator}(t) + Q_{electrolyte}(t) + Q_{anode}(t) + Q_{cathode1}(t) + Q_{cathode2}(t) \quad (2)$$

The heat generation rate $Q_x(t)$ [8] is calculated by

$$Q_x(t) = \Delta H_x \cdot m_x \cdot \frac{dc_x^d(t)}{dt} \quad (3)$$

$$\frac{dc_x^d(t)}{dt} = A_x \cdot [c_x(t)]^{n_{x,1}} \cdot [1 - c_x(t)]^{n_{x,2}} \cdot \exp(-\frac{E_{a,x}}{R \cdot T(t)}) \cdot g_x(t) \quad (4)$$

$$c_x(t) = c_0(t) - \int_0^t \frac{dc_x(t)}{d\tau} d\tau \quad (5)$$

$$\frac{dc_x(t)}{dt} = \frac{dc_x^d(t)}{dt} - \frac{dc_x^g(t)}{dt} \quad (6)$$

where the subscript x stands for different chemical reaction, d and g for decomposition and generation respectively. ΔH_x donates the reaction enthalpy, m_x is the total mass of the reactants, $c_x(t)$ is the normalized concentration of reactants, $g_x(t)$ is the correction term.

For SEI, the generated rate is proportional to decomposition rate of anode [8], given as

$$\frac{dc_{SEI}^g(t)}{dt} = K_{SEI}^g \cdot \frac{dc_{anode}^d(t)}{dt} \quad (7)$$

where the coefficient K_{SEI}^g is set as 1.5.

For anode, the term $g_{anode}(t)$ is calculated by

$$g_{anode}(t) = \exp(-\frac{c_{SEI}(t)}{c_{SEI,0}^{ref}}), c_{SEI,0}^{ref} = 1 \quad (8)$$

$Q_{ele}(t)$ can be obtained [8] by

$$Q_{ele}(t) = \frac{1}{\Delta t}(\Delta H_{ele} - \int_0^t Q_{ele}(t) d\tau) \quad (9)$$

$$\Delta H_{ele} = m \cdot C_p \cdot \Delta T - \Delta H_{chem} \quad (10)$$

where ΔH_{ele} represents the total electric energy left when short circuit occurs (triggered when temperature reaches 200°C), m is total weight of battery at 315g. ΔT is the total temperature increment from TR test, ΔH_{chem} is the total chemical reaction heat calculated by the integral of $Q_{chem}(t)$. The short circuit duration time is set at 24s. $Q_{vent}(t)$ represents the total heat released causing a temperature decrease of about 2.5 °C, and the duration time is set as 20s. Parameters used in TR modeling are listed in Tables 1 and 2.

Table 1. Parameters in TR model, part 1

x	m_x/g	$c_{x,0}$	$n_{x,1}$	$n_{x,2}$
SEI	44.78	0.15	1	0
anode	44.78	1	1	0
separator	7.84	1	1	0
cathode1	79.75	0.99	1	1
cathode2	79.75	0.99	1	1
electrolyte	48.09	1	1	0

Table 2. Parameters in TR model, part 2

Parameter	ΔH_x/J·g^{-1}	A_x/ s^{-1}	$E_{a,x}$/ J·mol^{-1}
SEI	257	1.3336E+14	1.3508E+05
anode	1714	0.18(<110℃) 0.5(>170℃)	3.4000E+04
separator	-233.2	3.0000E+51	4.2000E+05
cathode1	77	5.2500E+10	1.1495E+05
cathode2	84	7.2698E+10	1.1769E+05
electrolyte	800	6.7500E+15	1.7170E+05

2.3 TR Simulation and experimental validation

The TR simulation and experiment were firstly conducted for a single battery, triggered by an oven heating in an adiabatic rate calorimeter (ARC) and side heating by an electric heater, respectively, to determine the TR heat source, and the contact thermal resistance (R_{cont}) between the internal cell and external hard Al shell. Then TR propagation processes triggered by side heating (Fig. 1(a)) were modeled with equivalent thermal resistance (R_{eq}) between 5 tightly packed batteries, and validated by tests with 2 mm and 4mm thick epoxy resin board (0.46W·m^{-1}·K^{-1}) between batteries. Temperatures at 6 positions (Fig. 1(b)) in the center at half height were monitored with K-type thermocouples.

Numerical simulations of TR and its propagation were performed using the TR heat source built above, heating program by ARC and side heating from the test. Detailed physical parameters of battery used in simulation are shown in Table 3.

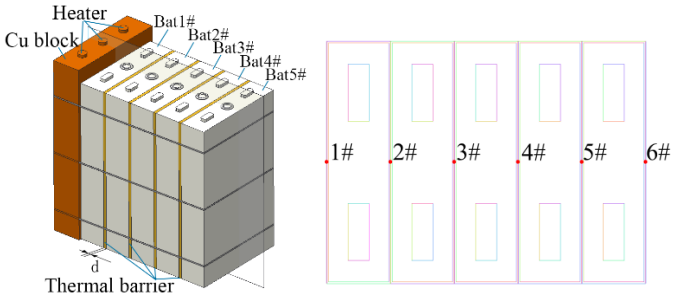

(a) (b)

Fig. 1 Diagram of battery module:3D(a), 2D(b)

Table 3. Physical parameters of LiB

Components	P(kg·m^{-3})	C_p(J·g^{-1}·k^{-1})	λ(w·m^{-1}·k^{-1})
cell	2255	1243	0.48/21 (perpendicular/ parallel to collector)
Al shell	2719	811	202.4

3. RESULTS AND DISCUSSION

3.1 Validation

TR of LiBs in adiabatic environments with "heat-wait-seek" mode was simulated. Fig. 2 shows the simulated temperature variations (sim) in comparison with results of ARC tests (exp). The simulated curve agrees well with experimental results, including the heat-wait-seek process (a) and vent opening process (b).

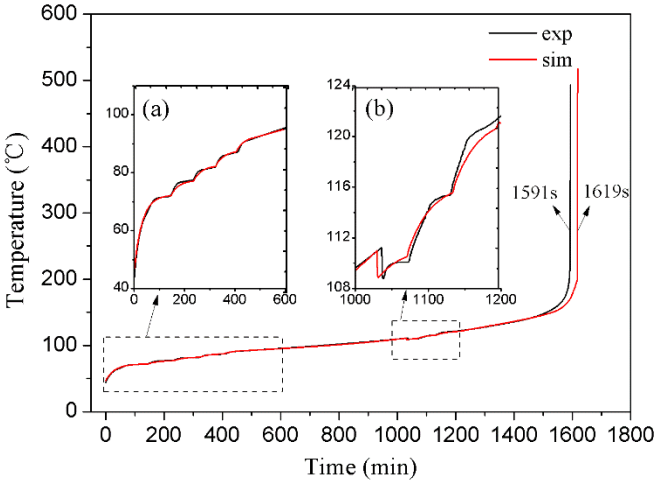

Fig. 2 Validation of TR heat source by ARC test

The TR model was also used to calculate temperatures of LiBs undergoing TR triggered by side heating. In this condition, the contact resistance R_{cont} between the internal cell and external Al shell of LiBs plays an important role. By minimizing the difference between simulated and experimental curves, R_{cont} could be deduced. Fig. 3 presents the comparison of temperature curves (at the center of heating surface (1#) and its opposite surface (2#)) between side heating TR test and simulation, in which R_{cont} is set equivalent to the air layer (0.0242 W·m^{-1}·K^{-1}) of 0.5 mm thickness. That means R_{cont} between internal cell and external Al shell of battery is around 0.0207 m^2·K·W^{-1}.

The heat transferred to the neighboring LiB from the triggered one caused TR propagation. Fig. 4 displays the average TR propagation time from the triggered LiB to the neighboring one. When no resistance (R_{eq}) was applied between batteries, simulated time intervals of TR propagation is shorter than the experiment, because contact resistance between batteries is impossible to be eliminated in the tests. Meanwhile, swell of LiBs and high temperature lead to the decrease of thermal resistance of epoxy resin board, resulting faster propagation in experiments. The simulation results of TR propagation captured most of the characteristics, and could be used for TR propagation mitigation design of LiB modules.

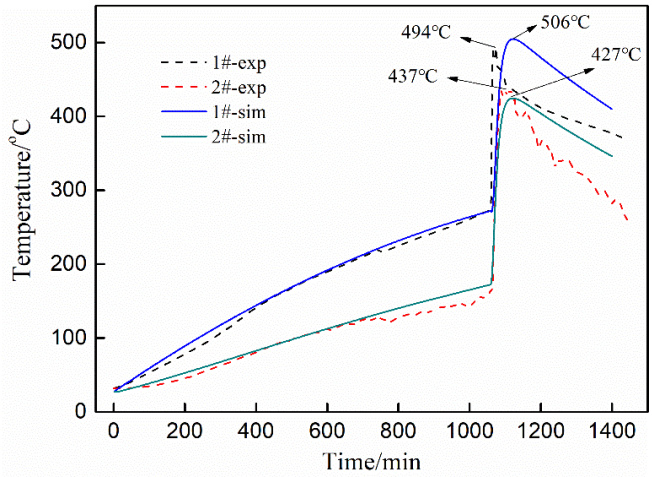

Fig. 3 Determination of R_{cont} by side heating test

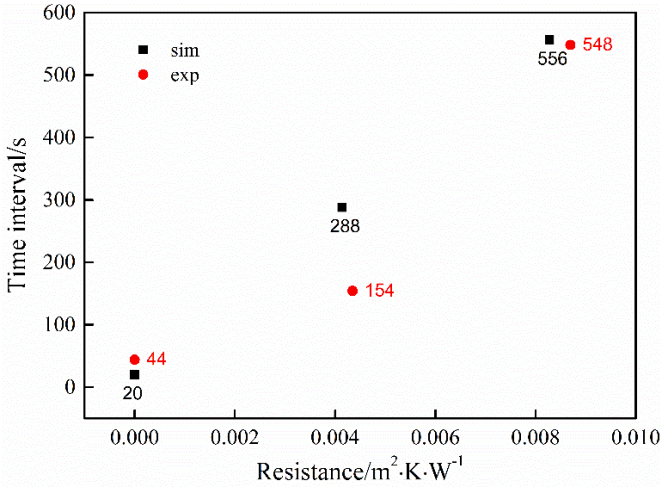

Fig. 4 Validation of total TR propagation time

3.2 Simulation of TR propagation with thermal barrier

Thermal barriers, equivalent to air layers of 0.1 mm (0.00414 m^2·K·W^{-1}), 0.2 mm (0.00828 m^2·K·W^{-1}), 0.3 mm (0.01242 m^2·K·W^{-1}) thickness of thermal resistance, were set between batteries, respectively. Temperature curves at locations (1# to 6#) during TR propagation process is shown in Fig. 5. Average TR propagation time for barrier with thickness of 0.1 mm, 0.2 mm, 0.3mm, is 20s, 296.5s, 603.5s per LiB, respectively. For barrier with 0.3 mm thickness, no TR propagation occurs after TR of the second battery. The time interval for TR propagation from the triggered one to the second battery, is up to 1356s.

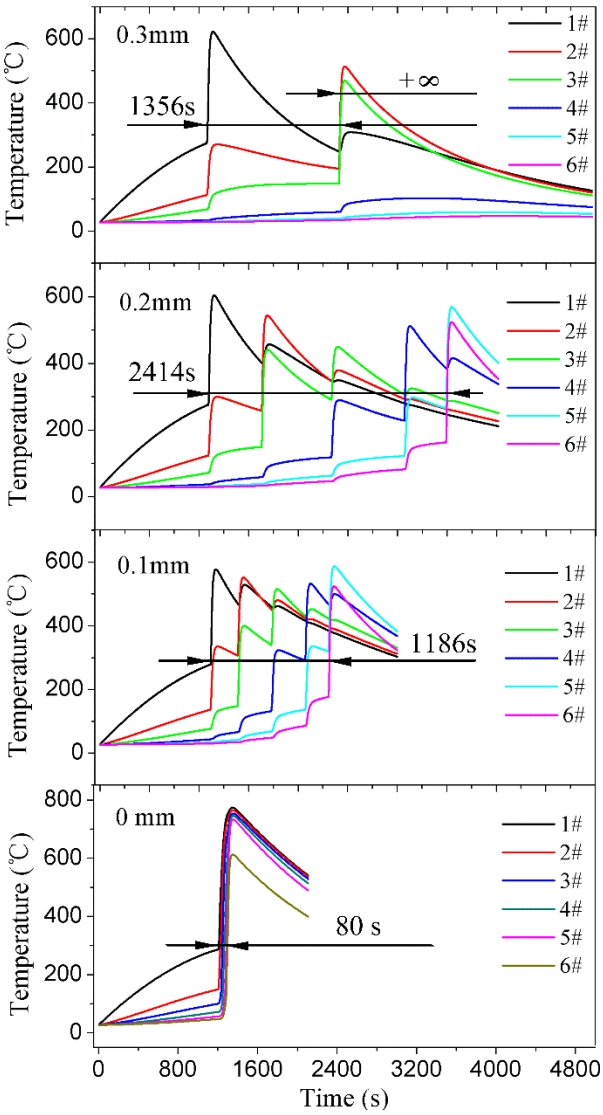

Fig. 5 Simulation of TR propagation process

Fig. 6 shows the detailed time intervals for TR propagating to neighboring batteries in modules with different R_{eq}. It can be observed that, for TR triggered by side heating, to extend TR propagation time interval to be more than 5 min, thermal resistance of barrier should be higher than 0.00414 $m^2 \cdot K \cdot W^{-1}$, and thermal resistance of 0.00828 $m^2 \cdot K \cdot W^{-1}$ could extend the TR propagation time to 10 min. A barrier with thermal resistance higher than 0.01242 $m^2 \cdot K \cdot W^{-1}$ is needed for preventing TR propagation.

4. CONCLUSION

A TR model considering contact thermal resistance between cell and hard shell of battery was built and used in the numerical simulation of TR propagation with thermal barrier between LiBs. The main conclusions are:

(1) A TR model including the consideration of contact thermal resistance between cells and hard shells was built, and verified by ARC and side heating tests.

(2) For the type of LiBs used in this work, the contact resistance between internal cell and external Al shell of battery is deduced to be around 0.0207 $m^2 \cdot K \cdot W^{-1}$.

(3) Numerical simulation of TR propagation revealed that the resistance of thermal barrier should be higher than 0.01242 $m^2 \cdot K \cdot W^{-1}$ to prevent TR propagation.

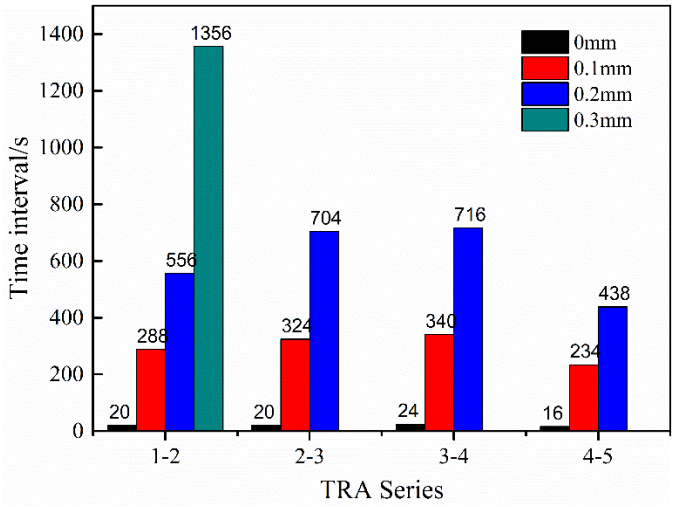

Fig. 6 TR propagation time interval between batteries

ACKNOWLEDGEMENT

This work is supported by the National Key R&D Program of China (2018YFB0104100).

REFERENCES

[1] Sun P, Bisschop R, Niu H, et al. A Review of Battery Fires in Electric Vehicles. Fire Technology. 2020;56:1361-410.

[2] Feng X, Ouyang M, Liu X, et al. Thermal runaway mechanism of lithium ion battery for electric vehicles: A review. Energy Storage Materials. 2018;10:246-67.

[3] Feng X, Sun J, Ouyang M, et al. Characterization of penetration induced thermal runaway propagation process within a large format lithium ion battery module. Journal of Power Sources. 2015;275:261-73.

[4] Feng X, Ren D, He X, et al. Mitigating Thermal Runaway of Lithium-Ion Batteries. Joule. 2020;4:743-70.

[5] Ping P, Wang Q, Huang P. Thermal behaviour analysis of lithium-ion battery at elevated temperature using deconvolution method. Applied Energy. 2014;129:261-73.

[6] Ping P, Wang Q, Chung Y. Modelling electro-thermal response of lithium-ion batteries from normal to abuse conditions. Applied Energy. 2017;205:1327-44.

[7] Ren D, Liu X, Feng X, et al. Model-based thermal runaway prediction of lithium-ion batteries from kinetics analysis of cell components. Applied Energy. 2018;228:633-44.

[8] Feng X, He X, Ouyang M, et al. Thermal runaway propagation model for designing a safer battery pack with 25Ah LiNixCoyMnzO2 large format lithium ion battery. Applied Energy. 2015;154:74-91.